Planta (1991) 186:2–12

Planta
© Springer-Verlag 1991

Transfer cells and solute uptake in minor veins of *Pisum sativum* leaves

Larry E. Wimmers* and Robert Turgeon**

Section of Plant Biology, Division of Biological Sciences, Cornell University, Ithaca, NY 14853, USA

Received 16 November 1990; accepted 16 July 1991

Abstract. Morphometric and physiological studies were conducted to determine whether the wall ingrowths of transfer cells in the minor-vein phloem of *Pisum sativum* L. leaves increase the capacity of the cells for solute influx. Size and number of wall ingrowths are positively correlated to the photon flux density (PFD) at which the plants are grown. An analysis of plasmodesmatal frequencies indicated that numerous plasmodesmata are present at all interfaces except those between the sieve-element–transfer-cell complex (SE-TCC) and surrounding cells where plasmodesmata are present but few in number. Flux of exogenous sucrose into the SE-TCC was estimated from kinetic profiles of net sucrose influx into leaf discs, quantitative autoradiography, and measurements of sucrose translocation. Flux based both on the saturable (carrier-mediated) and the linear components of influx was 47% greater in leaves of plants grown at high PFD (1000 $\mu mol \cdot m^{-2} \cdot s^{-1}$) than those grown in low PFD (200 $\mu mol \cdot m^{-2} \cdot s^{-1}$) and was paralleled by a 47% increase in SE-TCC plasmalemma surface area. Flux of endogenous photosynthate across the SE-TCC plasmalemma was calculated from carbon balance and morphometric data. The increase in flux in high-light leaves over that in low-light leaves can be explained on the basis of an increase in plasmalemma surface area. In intact leaves, a 'standing osmotic gradient' may facilitate transport of solute into transfer cells with extensive wall elaborations.

Key words: Phloem (loading, transfer cells) – *Pisum* (phloem transfer cells) – Plasmodesma (frequency) – Transfer cells (phloem)

Introduction

It is generally accepted that wall ingrowths of transfer cells increase the capacity for solute flux between the apoplast and symplast (Gunning and Pate 1969, 1974). This view is supported by three lines of circumstantial evidence: anatomical distribution, development, and cytochemistry. Transfer-cell locations generally coincide with sites of known or assumed high solute flux such as floral nectaries (Schnepf 1974; Kronestedt and Robards 1987), salt glands (Gunning and Pate 1969; Faraday and Thomson 1986), developing seeds (Gunning and Pate 1974; Maze and Lin 1975; Willemse and Kapil 1981; Folsom and Peterson 1984; Tilton et al. 1984; Folsom and Cass 1986), and the minor-vein phloem of source leaves (Gunning and Pate 1969, 1974; Pate and Gunning 1969; Watson et al. 1977; Kuo 1983; Scheirer 1983; Bourquin et al. 1990). The development of wall ingrowths begins with the onset of solute flux (Gunning and Pate 1969; Gunning et al. 1974; Kramer et al. 1978; Landsberg 1982; Folsom and Cass 1986). In *Pisum sativum* leaves, for example, the transfer cells of minor-vein phloem develop only after export of photoassimilate begins (Gunning et al. 1968; Peterson and Yeung 1975). Cytochemical evidence indicates that transfer cells are highly active metabolically; the numerous mitochondria may provide the energy required for active solute flux. Further, ATPase activity has been localized at the plasmalemma (Maier and Maier 1972; Hill 1975a, 1975b; Bentwood and Cronshaw 1978), and a transplasmalemma potential difference exists in haustorial transfer cells (Renault et al. 1989).

However, direct quantitative evidence correlating plasmalemma surface area with solute flux in transfer cells is lacking. This is undoubtedly a consequence, at least in part, of the difficulties involved in studying transport in complex tissues. In addition, for comparative purposes such studies require controls in which transfer cells have few, if any, wall ingrowths. To obtain quantitative and cell-specific solute-flux data, the experi-

* *Present address:* Department of Vegetable Crops, University of California, Davis, CA 95616, USA
** To whom correspondence should be addressed

Abbreviations: LPI = leaf plastochron index; PCMBS = *p*-chloromercuribenzenesulfonic acid; PFD(s) = photon flux density (densities); SE-TCC = sieve-element–transfer-cell complex

mental system must meet three requirements. First, solute movement across the transfer-cell plasmalemma must be discernible from that associated with other cell types. Second, symplastic exchange must be absent or minimal. Third, the degree of elaboration of the transfer-cell wall ingrowths must be experimentally controllable.

We are particularly interested in the role of transfer cells in phloem loading, i.e., the movement of photoassimilate from the mesophyll to the sieve elements of minor veins. It is generally assumed that the route of sucrose loading is at least partly apoplastic (for a review, see Giaquinta 1983) and that, in some species such as *Pisum sativum*, transfer-cell wall ingrowths facilitate uptake of sucrose from the free space (Gunning et al. 1968).

Pea leaves are an effective material for the study of transfer cells. While the phloem is complex, it is nonetheless open to direct analysis and manipulation: access to the free space is relatively easy, the vascular tissue is arranged in a two-dimensional reticulate network, and the phloem is relatively close to the surface, permitting quantitative analysis of the distribution of radiolabeled compounds in mesophyll and vascular tissues (Turgeon 1987). In this paper we demonstrate that the development of transfer-cell wall ingrowths in pea leaves may be experimentally modified. We also present a comprehensive morphometric analysis of parameters required for a quantitative study of solute-flux capacity, including plasmodesmatal frequencies. Finally, we demonstrate that phloem loading of both photoassimilates in intact leaves and exogenously supplied sucrose in leaf discs increase with increasing elaboration of transfer-cell wall ingrowths. These experiments provide direct evidence that wall ingrowths of transfer cells increase solute uptake by increasing plasmalemma surface area.

Material and methods

Plant material. Dwarf-pea plants (*Pisum sativum* L. cv. Little Marvel) were grown in 250-cm^3 plastic pots containing a mixture of peatmoss, perlite, and sterilized soil (2:1:1, by vol.) in a temperature-controlled room. Seeds were obtained from Agway, Syracuse, N.Y., USA. Illumination was provided 16 h per day with a combination of eight 40-W fluorescent and two 1000-W incandescent metal-halide lamps (M1000/c/v metalarc; Sylvania, Danvers, Mass., USA). All lamps were located 50 cm above plant level. Photon flux density (PFD) was controlled by shading the plants with cheesecloth suspended 25 cm above the top of the plants. Four PFDs were employed in some experiments (see figures) whereas in others only 'low-light' and 'high-light' (200 and 1000 μmol photons $\cdot m^{-2} \cdot s^{-1}$ respectively; photosynthetically active radiation) plants were compared. Air temperature was maintained at 20° ± 2° C during the day, and 14° ± 2° C at night. Air temperature at leaf level during the day was 21° ± 2° C under the highest, and 20° ± 2° C under the lowest, light conditions. At night the air temperature was uniform throughout the room. Air circulation within the room was provided by three fans; one pair for input and exhaust, and one circulation fan to improve air flow around the plants. The plants were watered daily with 20° C tap water, and fertilized weekly with a 0.03% solution of 20/20/20 water-soluble fertilizer (Peters Professional Water Soluble Fertilizer; W.R. Grace Co., Fogelsville, Penn., USA). The soil was covered loosely with aluminum foil to prevent the lamps from heating the soil to different degrees under different PFDs and to maintain uniform soil moisture levels. Soil temperature was 21° C at the highest, and 20° C at the lowest, PFD during the day; it was a uniform 14° C during the night. The leaf plastochron index (LPI) was calculated according to Erickson and Michelini (1957) using an index leaf length of 10 mm.

Microscopy. Mature laminae were cut into 2-mm^2 pieces and fixed in 4% (w/v) glutaraldehyde in 0.07 M sodium-cacodylate buffer, pH 7.0, for 4 h at 23° C. The tissue was washed in buffer, postfixed in 2% (w/v) OsO_4 for 2 h at 23° C, washed in buffer again, stained in 2% (w/v) uranyl acetate for 20 min, dehydrated in ethanol, and embedded in Spurr resin (Spurr 1969). Thin sections (50–80 nm) were cut with a diamond knife and stained with lead citrate and uranyl acetate. Grids were viewed and photographed on a Phillips (Eindhoven, The Netherlands) 201 transmission electron microscope. Thick sections (1.0 μm) were stained with 1% (w/v) Toluidine blue for light microscopy and photographed with a Leitz Ortholux microscope (Rockleigh, N.J., USA).

For quantification of cell-wall-perimeter length, cell-contact lengths, and plasmodesmatal frequency, transverse sections of 80 minor veins, 20 each from four different PFDs (four different plants within each PFD) were photographed at low magnification (× 3000) and the transfer cells of those veins were photographed again at medium magnification (× 7000–10000). Micrographs were projected at × 3 magnification onto a ZIDAS digitizer board (Carl Zeiss, Thornwood, N.Y., USA). Low-magnification micrographs of entire veins were used to determine the length of interface between various cell types and to count plasmodesmata. As noted previously (Gunning and Pate 1969), the plasmalemma of transfer cells frequently appears to have separated from the cell wall, leaving an electron-translucent space. This is especially common around the wall ingrowths, and is generally considered to be an artifact of fixation. Measurements of the internal cell-wall perimeter are, therefore, probably a better indicator of original plasmalemma-perimeter length than those obtained from the retracted plasmalemma itself. Plasmodesmatal frequency between cell types was calculated according to Robards (1976), compensating for section thickness and radius of the plasmodesmata.

To quantify vein length, and to analyze the anatomy of veins of different sizes, it was necessary to develop a method in which individual veins could be viewed paradermally and in cross section. Large pieces of lamina (25 mm^2) were cut and cleared in a 3:1 (v/v) mixture of 95% ethanol and glacial acetic acid at 23° C overnight. The tissue was viewed and photographed paradermally with phase-contrast optics using a × 4 objective. The tissue was cut transversely with a sharp razor blade and re-photographed. The veins at the newly cut edge could then be viewed in cross section and their position in the vein network determined from the paradermal view photographed before the cut was made. To obtain cross sections the tissue was dehydrated in an alcohol series, embedded in Spurr resin, and positioned in flat molds so that the newly cut edge could be sectioned. Thick sections were cut and stained as above for light microscopy.

Statistical analysis. All parameters are reported as the average of at least ten samples; the exact numbers of samples are indicated in the figure legends. Each sample represents the average of measurements made on four minor veins and surrounding cells from a single leaf. Cell-wall-perimeter lengths, cell cross-sectional areas, and vein lengths at different PFDs were compared using the Student *t*-test with a 95% confidence interval.

Plasmodesmatal frequencies were not normally distributed since plasmodesmata tend to occur in aggregates. Therefore, thin sections exhibit a wide range of plasmodesmatal frequencies with a disproportionate number of samples grouped at or near zero. Because of this non-parametric distribution, the Kruskal-Wallis one-way analysis of variance by ranks, with a 95% confidence interval, was used to compare frequencies between high and low PFDs and between different cell interfaces (Daniel 1978).

Net carbon exchange. Net carbon exchange of leaf 5 was measured by infra-red gas analysis at a flow rate of 2 L $\cdot min^{-1}$. The plant

was allowed to equilibrate for 1 h before the system was closed and measurements were begun. Air temperature within the assimilation chamber was 22° ± 1° C. Relative humidity was maintained at a dew point of 12° C.

Translocation rate. The average translocation (export) rate (TR) was calculated by the equation:

$$TR = ([DC \cdot DS] + [NC \cdot NS] - WC) \cdot (DS + NS)^{-1} \cdot CS^{-1}$$

where DC and NC are the average net carbon-exchange rates during the light and dark periods, respectively, measured in mol $CO_2 \cdot s^{-1} \cdot cm^{-2}$; DS and NS are the lengths of the light ($5.76 \cdot 10^4$ s) and dark ($2.88 \cdot 10^4$ s) periods, respectively; WC is the average dry-weight change per 1 cm^2 of leaf area (at LPI 3.0) over a 24-h period, and CS is the number of carbon atoms per sucrose molecule. No dry-weight change was detected. The equation can be further simplified by cancelling numerical values:

$$TR = (2DC + NC) \cdot 36^{-1}$$

Theoretical fluxes. The transmembrane flux of photoassimilates (PF) (flux across the plasmalemma of the sieve-element–transfer-cell complex (SE-TCC), assuming an entirely apoplastic loading route) was calculated by the equation:

$$PF = TR \cdot PM^{-1}$$

where PM is the total area of the SE-TCC plasmalemma ($m^2 \cdot cm^{-2}$ leaf area) of Class III and IV veins.

The transmembrane flux of exogenously supplied sucrose into the minor-vein phloem (EF) was calculated (again assuming an entirely apoplastic route of entry into the SE-TCC) as:

$$EF = S \cdot VP \cdot PM^{-1}$$

where S is the rate of net sucrose influx ($mol \cdot s^{-1} \cdot cm^{-2}$ leaf area), and VP is the percentage of label in the minor veins (as opposed to that in the surrounding mesophyll tissue).

Translocation of [^{14}C]sucrose. Plants were brought into a laboratory fumehood illuminated by a water-filtered incandescent 1000-W metal-halide lamp providing approx. 1000 $\mu mol \cdot m^{-2} \cdot s^{-1}$ at plant level. A small area (approx. 8 mm diameter) of the adaxial surface of the leaf was abraded with carborundum (320 grit) for 30 s, rinsed briefly with distilled water, patted dry, and a small (8 mm inside diameter, 5 mm deep) well cut from flexible plastic tubing was attached over the abraded area with a thin bead of lanolin paste. The well was filled with 200 µl 2(N-morpholino)ethanesulfonic acid buffer (20 mM Mes plus 20 mM $CaCl_2$ adjusted to pH 5.5 with KOH) + 10 mM [^{14}C]sucrose ($4 \cdot 10^{10}$ Bq $\cdot$ mol^{-1}) while the leaf was supported in its normal position with a wire-mesh screen. In some plants a red-hot dissection probe was used to scald the petiole of the labeled leaf and thereby kill the phloem tissue. When this was done the leaf remained completely turgid during the following 2 h.

Label was applied for 1 h, after which the radiolabeled sucrose solution was removed and the well washed by five quick changes of buffer solution before refilling the well with buffer + 25 mM unlabeled sucrose. After a 1-h chase period the well was removed and a 1-cm-diameter disc including the abraded area was excised with a cork borer. The disc was floated in buffer solution for a total of 35 min with buffer changes (22° C) on a schedule of 1-, 5-, and 15-min intervals to remove free-space label. Meanwhile, varous parts of the plant were prepared directly for liquid scintillation counting by the method of Sun et al. (1988). The nonlabeled mature source leaves and the roots were frozen in liquid nitrogen, ground to a fine pulp, lyophilized at 30° C (Virtis freeze-dryer: Virtis Co., Gardiner, N.Y., USA) and weighed before scintillation counting of representative weighed samples.

[^{14}C]Sucrose uptake into leaf discs. Mature leaves (leaf 4 or 5, LPI 2.5–3.0) were abraded and 5.6-mm diameter discs were removed with a cork borer under the surface of Mes buffer (22° C). In most cases (exceptions are noted in *Results*) at least five leaves (one from each plant) were used to provie 20 discs per treatment. Discs were randomized and transferred to the surface of fresh buffer (22° or 1° C) in small (3.5 cm diameter) plastic Petri dishes. The buffer was removed and replaced with 2.5 ml of solution containing Mes buffer + [^{14}C]sucrose at 22° C or 1° C for periods ranging from 10 min to 2 h. The concentration of [^{14}C]sucrose was 10 mM, except where noted, and the specific activity was $1 \cdot 10^8$ Bq $\cdot$ mol^{-1} except where noted.

At the end of the uptake period the [^{14}C]sucrose solution was quickly removed and the discs were washed with buffer (22° or 1° C) for 35 min. Changes of buffer wash were made on a schedule of 1-, 5-, and 15-min intervals.

Autoradiography. Leaf discs were frozen in powdered solid CO_2, lyophilized, and autoradiographed. Details of these, and quantitative autoradiography, procedures are given in Turgeon (1987).

Results

Leaf anatomy. A morphometric analysis of leaves grown under low and high light (200 and 1000 µmol photons $\cdot$ $m^{-2} \cdot s^{-1}$) conditions was conducted to provide the quantitative data required for estimates of solute flux. Overall leaf thickness is greater, intercellular spaces smaller, and leaf area (18.4 cm^2 versus 23.0 cm^2) smaller, in plants grown at high PFD. Low- and high-light leaves have one and two layers of palisade cells, respectively, and two and four layers of spongy cells, respectively. Total mesophyll volume in high-light leaves is 47% greater than in low light leaves (47 and 32 $mm^3 \cdot cm^{-2}$ leaf area, respectively).

Since vein order, as determined by branching patterns, is a poor indicator of vein size and anatomy, veins were grouped into four classes on the basis of width (Table 1). Class III and IV veins delimit the majority of areoles and form the blind endings within them, and are therefore defined as minor veins.

Vein anatomy. Minor-vein anatomy is similar to that described by Gunning and Pate (1968) for *P. arvense*. Minor veins are collateral, consisting of a variable number (one to five) of tracheary elements with or without xylem parenchyma, sieve elements with associated transfer cells, phloem parenchyma, and a chlorenchymatic bundle sheath entirely enclosing even the smallest veins (Fig. 1). There is no consistent orientation of the SE-TCC within the vein; in reference to its transfer cell, the sieve element is as often peripheral as it is internal and as often abaxial as it is adaxial. Sieve elements and transfer cells both abut phloem-parenchyma and bundle-sheath cells. Sieve elements are always juxtaposed to at least one transfer cell, and there are frequently more transfer cells than sieve elements. Interfaces between transfer cells are common. Contact between sieve elements also occurs but is less common. Individual SE-TCCs may be in direct contact or phloem parenchyma may be present between them. Phloem parenchyma is always present and each of these cells abuts at least one bundle-sheath cell as well as sieve elements and transfer cells. Phloem-parenchyma cells protrude from the bundle sheath into, and often across, the vein; thus the vein

Table 1. Morphometric analysis of four vein classes in mature *Pisum sativum* source leaves. Plants were grown under low or high (200 or 1000 μmol photon·m^{-2}·s^{-1}, respectively) PFDs. Vein width and length were measured in cleared tissue. Number of sieve elements were determined in 1-μm cross sections. Sieve-element and transfer-cell cross-sectional areas were measured in electron micrographs of thin sections ($n=50$). Phloem volume was calculated as the product of vein length, number of sieve elements and transfer cells, and their cross-sectional area. ±Values = SE

Vein class	Vein width (μm)	No. of sieve elements	Vein length (mm·cm^{-2})		Sieve-element area (μm^2)		Transfer-cell area (μm^2)		Phloem volume ($mm^3 \cdot cm^{-2} \times 10^{-3}$)		Phloem volume (%)	
			High light	Low light	High light	Low light	High light	Low light	High light	Low light	High light	Low light
I	180	≥9	12.4 ±2.2	8.8 ±1.3	10.0 ±1.1	9.9 ±1.2	30.6 ±1.9	28.9 ±1.9	0.3	0.2	7.0	5.0
II	90–179	7–9	23.5 ±1.8	24.0 ±2.1	8.2 ±0.9	8.3 ±0.9	34.3 ±2.3	33.1 ±2.1	0.8	0.8	18.6	20.0
III	45–89	4–7	36.0 ±2.3	43.2 ±3.7	7.0 ±0.6	7.0 ±0.5	38.2 ±2.3	37.5 ±3.1	0.9	1.1	20.9	27.5
IV	20–44	1–4	159.2 ±10.3	141.7 ±12.1	6.5 ±0.5	5.9 ±0.5	41.8 ±3.0	39.6 ±3.0	2.3	1.9	53.5	47.5
			230.7	218.0					4.3	4.0		

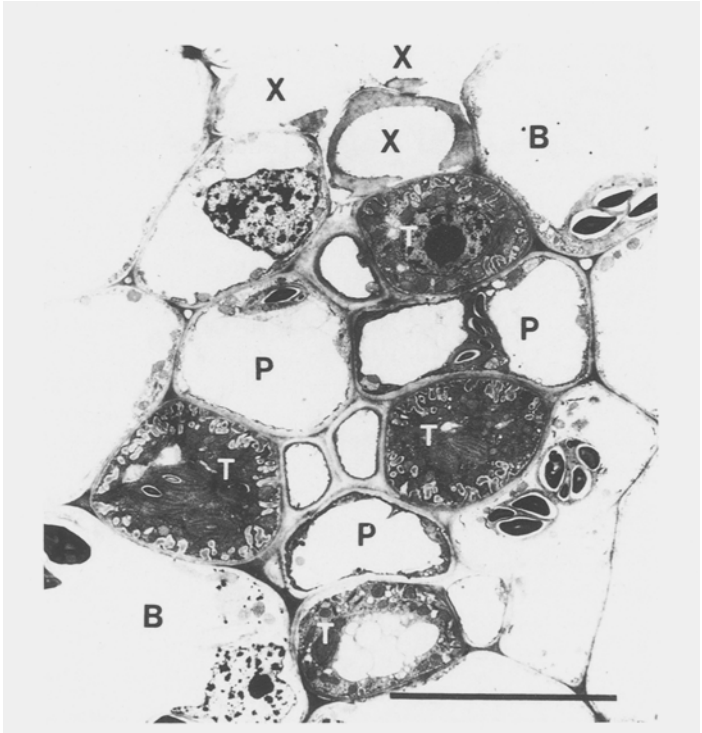

Fig. 1. Electron micrograph of a cross-section of a minor vein in mature lamina tissue of *P. sativum*. Tracheary elements (*X*), phloem parenchyma (*P*), bundle-sheath cells (*B*), and transfer cells with associated sieve elements (*T*). Scale = 10 μm; ×3000

has a tiered appearance, phloem parenchyma in alternate rows with the SE-TCCs (Fig. 1).

Larger veins (Classes I and II) are composed of the same cell types as the smaller veins. In these veins the SE-TCC orientation is more predictable. Sieve elements may occur above or below their transfer cells (where they may abut bundle-sheath cells), but are usually located on the side toward the center of the vein, and are never located external to transfer cells. The number of transfer cells and sieve elements is equal and individual complexes are not usually in direct contact. Phloem-parenchyma cells are found between the complexes.

Ultrastructure of transfer cells. The transfer cells of minor veins of *P. sativum* leaves have been described by Bentwood and Cronshaw (1978). According to Gunning and Pate (1969) these are "A" type transfer cells, that is they are primarily associated with the phloem, and wall ingrowths are found along the enitre perimeter except that relatively few are seen in the portion of the wall abutting the sieve element. Wall ingrowths are finger-like projections averaging 0.2 μm in diameter, and ranging up to 2 μm in length (Fig. 2). Ingrowths bend and frequently fuse, especially in minor veins of high-light leaves.

There is a positive correlation between the perimeter length of tranfer-cell walls and the PFD under which the plants are grown (Figs. 2 and 3). This is most apparent in Class IV veins (Fig. 3). Both number and length of ingrowths increase with increasing PFD.

Plasmodesmata frequency. All plasmodesmata, except those between transfer cells and sieve elements, are unbranched; they occur either singly or in aggregates. Lateral sieve areas, not plasmodesmata, occur between contiguous sieve elements.

Cell interfaces fall into three broad groups based on plasmodesmatal frequencies (Table 2). Frequencies between groups are statistically different; those within groups are not. The highest plasmodesmatal frequencies are found between sieve elements and transfer cells, and between pairs of phloem-parenchyma cells. Lowest frequencies are seen at interfaces between the SE-TCC and surrounding cells.

Uptake of exogenous sucrose. Concentration dependence of [^{14}C]sucrose uptake into leaf discs of both low- and high-light plants is biphasic, as in many other systems (Giaquinta 1983), consisting of a high-affinity saturable

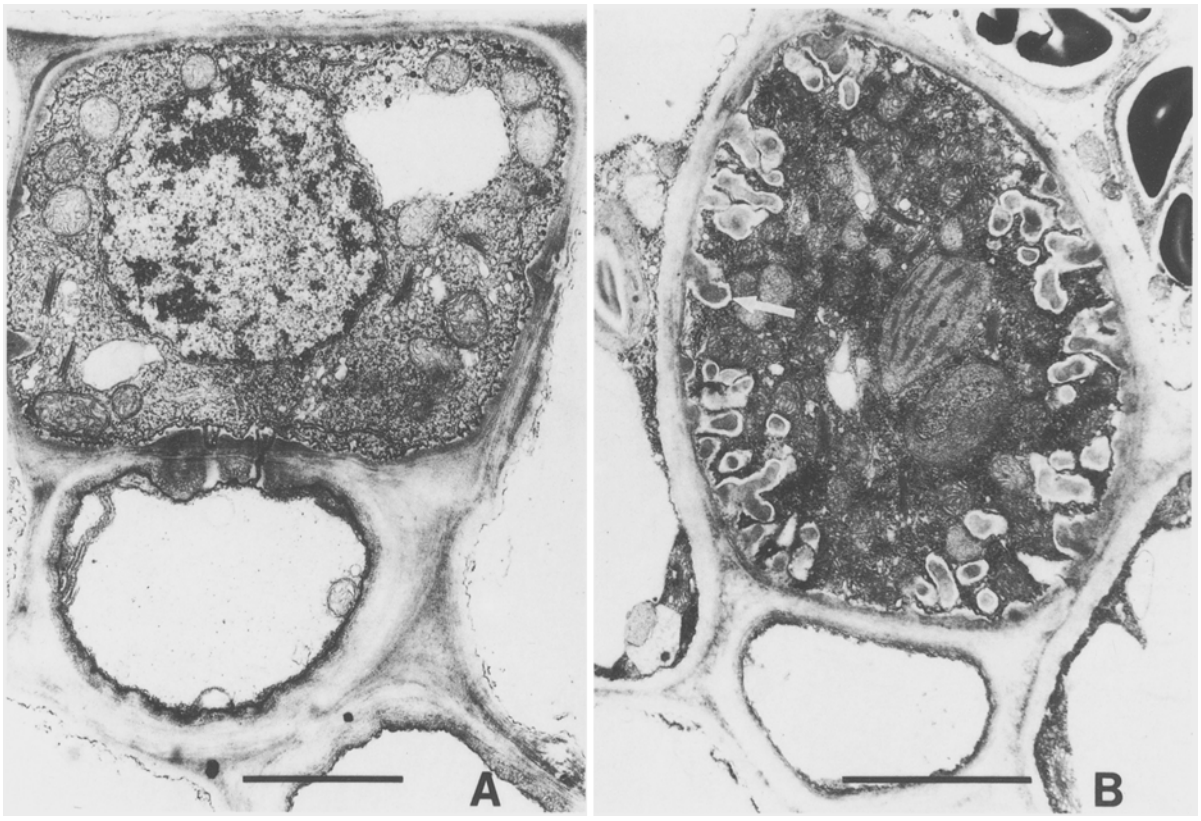

Fig. 2A, B. Electron micrographs of transfer cells of minor veins in mature lamina tissue of *P. sativum*. Plants grown at 200 **A** or 1000 μmol·m^{-2}·s^{-1} **B**. *Arrow* indicates electron-translucent area between plasmalemma and wall protuberance. Note the more extensive wall ingrowths in transfer cells of the high-light plants. Scale = 2.0 μm; ×12500 **A**, ×10500 **B**

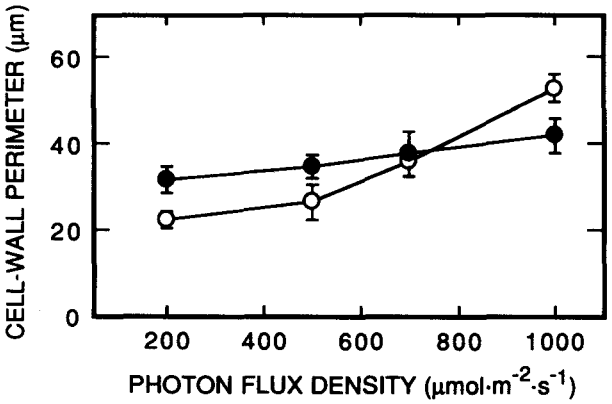

Fig. 3. Length of cell wall in transfer cells of mature leaves of *P. sativum* plants grown at different PFDs. ●—●, Class III veins (four to seven sieve elements); ○—○, Class IV veins (one to three sieve elements)

Table 2. Plasmodesmatal frequencies between cell types expressed on the basis of linear interface and area of interface. Frequencies with different superscripts are significantly different (Kruskal-Wallis one-way analysis of variance, 95% confidence interval, $n = 16$)

Interface	Plasmodesmata ·μm^{-1}	μm^{-2}
Transfer cell–sieve element	0.31^{a}	2.23
Phloem parenchyma–phloem parenchyma	0.31^{a}	2.23
Bundle sheath–mesophyll	0.14^{b}	1.01
Phloem parenchyma–bundle sheath	0.13^{b}	0.94
Mesophyll–mesophyll	0.11^{b}	0.79
Transfer cell–transfer cell	0.10^{b}	0.72
Bundle sheath–bundle sheath	0.09^{b}	0.64
Transfer cell–phloem parenchyma	0.05^{c}	0.35
Transfer cell–bundle sheath	0.03^{c}	0.21
Sieve element–phloem parenchyma	0.01^{c}	0.07
Sieve element–bundle sheath	0.00^{c}	0.00

component and a lower affinity, apparently non-saturable phase (not shown). Uptake of [^{14}C]sucrose (10 mM) into abraded leaf discs is positively correlated to PFD provided during growth (Fig. 4). Discs from high-light (10^3 μmol photons·m^2·s^{-1}) plants accumulate sucrose at a rate approx. 50% greater than discs from low-light (200 μmol photons·m^{-2}·s^1) plants. The rate of uptake is linear for 2 h and is not significantly influenced either by PFD provided during the uptake period, the osmotic potential of the uptake medium (0–200 mM mannitol), or the time of day (or night) at which the experiments were performed in discs from either high- or low-light plants (data not shown).

The apparent rate constant (k) of the linear phase was determined by linear regression of the last four points in each curve (Table 3) and the K_m and V_{max} were calculated from Lineweaver-Burke plots of the saturable component (Table 3). Uptake during linear phase is

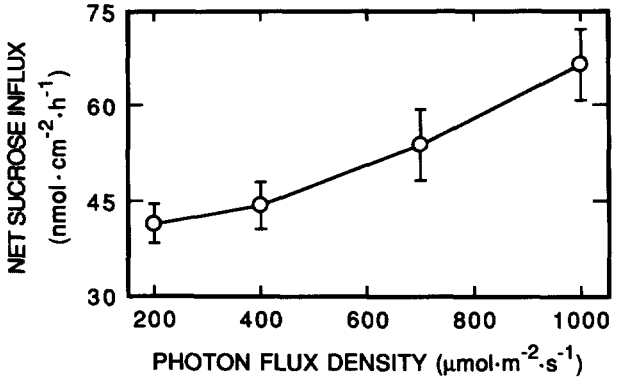

Fig. 4. Net sucrose influx into leaf discs from pea plants grown at different PFDs. Leaf discs cut from abraded mature leaves were floated on 10 mM [^{14}C]sucrose for 30 min, and washed for 35 min, before counting

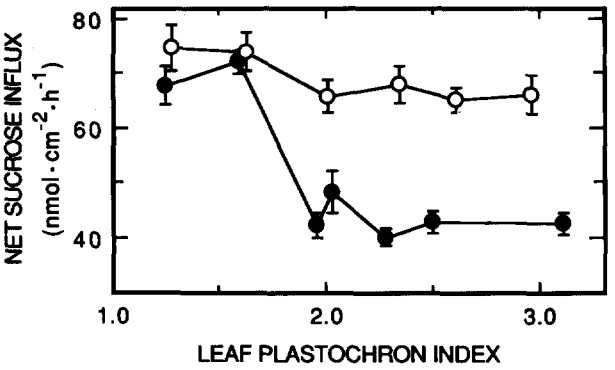

Fig. 5. Net sucrose influx into discs from pea leaves of increasing age. Discs were cut from abraded leaves of high-light (○—○) or low-light (●—●) plants and were floated on 10 mM [^{14}C]sucrose. One plastochron equals approx. 3 d. Leaves reach 50% and 100% of final area at approx. LPI 1.2 and LPI 2.0, respectively. Each datum point is the mean of ten discs from a single plant. Bars = SE

Table 3. Kinetic parameters of [^{14}C]sucrose uptake in leaf discs of pea leaves grown under low-light or high-light conditions

Component		Low light	High light
Saturable	K_m (mM)	19	19
	V_{max} (nmol·cm^{-2}·h^{-1})	95	148
Linear	k (nmol·cm^{-2} ·(mM sugar)$^{-1}$·h^{-1})	14	20

greater in discs of high-light polants than in discs of low-light plants. The K_m values for the saturable component is the same in low- and high-light plants while V_{max} is approx. 55% higher in high-light plants. The rate of sucrose influx depends on leaf age (Fig. 5). No difference in uptake is detected between discs of high- and low-light leaves until after LPI 1.5. The uptake in discs from both low- and high-light plants declines between LPI 1.5 and 2.0. A greater decline in uptake in discs from low-light plants accounts for the difference in uptake seen in mature leaves. Uptake is relatively constant between LPI 2.0 and 3.0. The sink-source transition (Turgeon 1989) occurs at LPI 1.5-1.8 and the leaves reach full expansion at LPI 2.0–2.2 (data not shown).

To determine whether rates of uptake were stable after leaves had matured, plants were moved from high to low PFD or vice versa and uptake was measured over the next 9 d. Uptake rates were stable for 6 d with some evidence of change in response to the new light conditions by the ninth day (not shown).

Vein loading and translocation of exogenous sucrose. Since influx of sucrose occurs into mesophyll as well as minor veins, it was necessary to estimate the proportion of label accumulated by the latter. This was done by analysis of autoradiographs. Distinct minor-vein images are apparent in autoradiographs of both low- and high-light discs after 30 min of uptake. The percentage of label in the minor veins was calculated from measurements of label density and surface area occupied by the veins. The ratio of label in the veins and in the interveinal regions (V/I) was determined by microdensitometry (Turgeon 1987) in three separate experiments. This ratio was not significantly different in autoradiographs of discs from low- and high-light plants (Table 4). Vein area (Table 4) was measured with a digitizer board in photographic enlargements made from the autoradiographs. These vein-area measurements do not represent the true area of the veins in the tissue since there is considerable enlargement caused by scatter of β-particles; however this is a reasonable method of determining the percentage of label in the veins, which is the same in both low- and high-light plants (66–67%).

To determine how much of the label in the minor veins entered the conducting elements of the phloem, the percentage of exogenous sucrose translocated out of the leaf was measured. [^{14}C]Sucrose (10 mM) was applied in a well to a small (8 mm diameter) abraded area of the upper side of an attached mature leaf for 1 h followed by a 1-h chase with unlabeled sucrose (10 mM). Label was measured in the dissected parts of the plant at the end of the chase period. The abraded area of the labeled leaf was removed separately and washed for 10 min before counting to remove label from the free space. The percentage of the label present in various parts of the plant is summarized in Table 5. Seventy percent of the label is exported from the treated leaf, a value that is close to the 66–67% value of label found in minor veins after uptake of [^{14}C]sucrose into leaf discs (Table 4). To be certain that label leaving the leaf was travelling in the phloem, the petiole of the treated leaf was heat-girdled in some experiments or *p*-chloromercuribenzene sulfonic acid (PCMBS) (2 mM) was included in the uptake solution; both treatments prevented export (not shown).

Calculations were made of the flux of sucrose across the plasmalemma of the SE-TCC assuming that all label in the minor veins entered the conducting elements of the phloem, i.e., the SE-TCC (see previous section). The further assumption was made that symplastic loading played a negligible role and, therefore, that all loaded sucrose crossed the SE-TCC plasmalemma.

Table 4. Distribution of ^{14}C in veins and interveinal tissue of *Pisum sativum* source leaves following uptake of [^{14}C]sucrose. Leaf discs cut from abraded mature leaves of low- or high-light plants were floated on 10 mM [^{14}C]sucrose for 30 min and washed for 35 min before freezing and lyophilization. Autoradiographs of dried, pressed discs were used for microdensitometry measurements (V/I; ratio of ^{14}C in veins and interveinal space) and enlarged prints of autoradiographs were used to determine vein area. The percentage of total label in the veins was calculated from V/I and vein-area data. Means from three experiments ± SE

	V/I	Vein area (%)	Vein label (%)
High light	3.3 ± 0.3	37.9 ± 4.2	67%
Low light	3.5 ± 0.3	35.2 ± 3.3	66%

Table 5. Percent of label in different parts of a pea plant after [^{14}C]sucrose (10 mM) was applied to a mature source leaf for 1 h followed by a chase with unlabeled sucrose (25 mM) for 1 h. Average of three experiments, ± SE

Organ	% of label in plant
Labeled leaf	30.0 ± 7.4
Petiole of labeled leaf	1.8 ± 0.2
Stem	5.3 ± 0.4
Immature leaves (LPI 0.0–1.0)	15.6 ± 1.4
Apex	0.7 ± 0.1
Roots	45.9 ± 2.2

These calculations indicate that, although leaf discs from high-light plants take up considerably more sucrose than discs from low-light plants, flux (per unit area of SE-TCC plasmalemma surface area) is very similar (Fig. 6). At low concentrations flux is the same; as sucrose concentration increases, flux is slightly greater in low-light leaves. These calculations indicate that the higher values of sucrose uptake into the SE-TCC of minor veins of high-light plants is paralleled by a proportional increase in the surface area of the SE-TCC plasmalemma.

Vein loading and translocation of photoassimilate. Measurements of net carbon exchange (NCE) were used to calculate translocation, and thus phloem-loading, rates in low- and high-light plants. Below 600 μmol photons · $m^{-2} \cdot s^{-1}$, NCE is the same in both groups (Fig. 7). At higher PFDs the NCE of low-light leaves reaches a plateau while that of high-light leaves continues to increase (Fig. 7).

Net carbon exchange of high-light plants is approx. 3.5 times as high, at ambient PFD (1000 μmol · $m^{-2} \cdot s^{-1}$), as the NCE of low-light plants at their ambient PFD (200 μmol · $m^{-2} \cdot s^{-1}$) (Fig. 8). These rates remained the same throughout the day, as did the rates of respiration during the night (replicate measurements made on leaves of three plants at hourly intervals; data not shown).

Total NCE over the 24-h period was calculated and used to determine average translocation rates (Table 6). Since leaf dry weight did not change significantly from one day to the next it was assumed that NCE over the 24-h period equalled the amount of carbon exported during the same period. Calculations were made in moles of sucrose since sucrose is the primary transport sugar in pea (Pate 1966). The average translocation rate is 3.7 times greater in high-light plants than in low-light plants.

Flux across the SE-TCC plasmalemma in low- and high-light plants was calculated using values for photoassimilate translocation (Table 6) and SE-TCC plasmalemma surface area (Fig. 3). Again, as in the calculations of exogenous sucrose flux (previous section), the

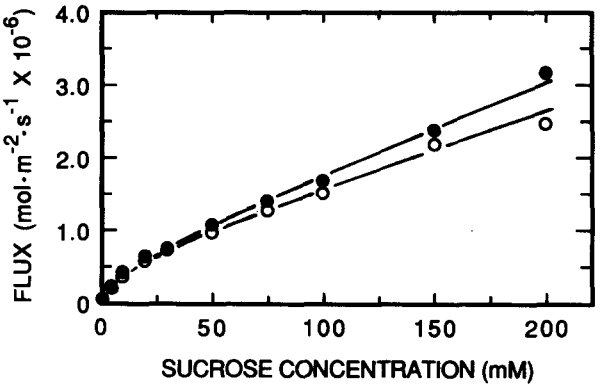

Fig. 6. Calculated transmembrane flux of exogenously supplied sucrose across the plasmalemma of the SE-TCC of class III and IV veins in low-light (●—●) and high-light (○—○) pea plants. Flux was determined assuming entirely apoplastic phloem loading

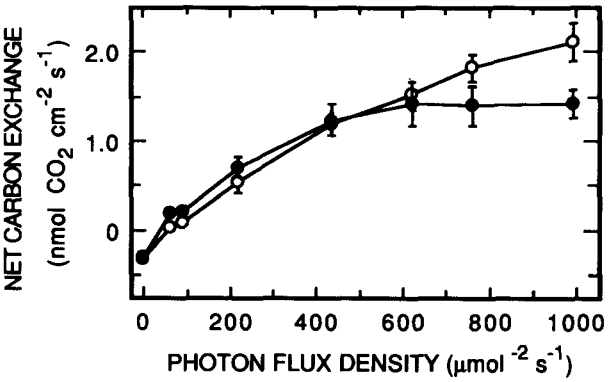

Fig. 7. Rates of net carbon exchange in whole, attached pea leaves at different PFDs for both low- (●—●) and high- (○—○) light plants. Mean values from four experiments. Bars = SE

Table 6. Calculated sucrose translocation rates and flux of sucrose in pea leaves across the plasmalemma of the SE-TCC, based on measurements of net carbon exchange. Translocation rates are averaged over a 24-h period and are expressed as mol sucrose · s^{-1} · (cm leaf area)$^{-2}$. Transmembrane flux was calculated assuming negligible symplastic phloem loading and is expressed as mol sucrose · s^{-1} · (m^2 SE-TCC plasmalemma surface area)$^{-1}$

	Translocation rate	Transmembrane flux
Low-light plants	$32.0 \cdot 10^{-11}$	$1.37 \cdot 10^{-6}$
High-light plants	$1.17 \cdot 10^{-10}$	$2.93 \cdot 10^{-6}$

Table 7. Six species ranked in order of decreasing plasmodesmatal frequency at the companion-cell–phloem-parenchyma, and companion-cell–bundle-sheath interfaces. Both absolute frequences (plasmodesmata per linear μm of interface) and relative frequencies (phloem parenchyma–phloem parenchyma = 1.0) are given. Data are from the following: *Amaranthus retroflexus* (Fisher and Evert 1982), *Beta vulgaris* (Evert and Mierzwa 1986), *Coleus blumei* (Fisher 1986), *Pisum sativum* (this paper), *Populus deltoides* (Russin and Evert 1985), *Vicia faba* (Bourquin et al. 1990)

Companion cell–phloem parenchyma				Companion cell–bundle sheath			
Absolute frequency	Species	Relative frequency	Species	Absolute frequency	Species	Relative frequency	Species
0.40	*P. deltoides*	1.69	*C. blumei*[a]	1.33	*C. blumei*[a]	8.30	*C. blumei*[a]
0.27	*C. blumei*[a]	0.75	*B. vulgaris*	0.73	*P. deltoides*	1.06	*P. deltoides*
0.25	*A. retroflexus*	0.63	*C. blumei*[b]	0.11	*A. retroflexus*	0.38	*B. vulgaris*
0.12	*B. vulgaris*	0.58	*P. deltoides*	0.06	*B. vulgaris*	0.18	*A. retroflexus*
0.10	*C. blumei*[b]	0.42	*A. retroflexus*	0.03	*P. sativum*	0.12	*V. faba*
0.05	*P. sativum*	0.16	*P. sativum*	0.01	*C. blumei*[b]	0.06	*C. blumei*[b]
0.003	*V. faba*	0.07	*V. faba*	0.005	*V. faba*	0.06	*P. sativum*

[a] Intermediary cell
[b] 'Ordinary' companion cell

assumptions were made that symplastic phloem loading is negligible and that only the minor veins (Class III and IV veins) are involved in loading. The calculations indicate that flux across the SE-TCC plasmalemma is approximately twice as high in high-light plants as in low-light plants (Table 6).

The concentration of exogenous sucrose that yields an SE-TCC transmembrane flux equivalent to that of photosynthetically-derived sucrose is 50 mM in low-light plants and in excess of 200 mM for high-light plants (compare Table 6 and Fig. 6).

Discussion

The purpose of these experiments was to test directly the hypothesis that transfer-cell wall ingrowths increase the capacity for solute flux by expanding the surface area of the plasmalemma. Pea minor veins are suited to this objective because uptake can be quantified by a number of techniques including scintillation counting of whole tissues, quantitative autoradiography, and translocation. Furthermore, the relative paucity of plasmodesmata connecting the SE-TCC to surrounding cells, in comparison to species in which the companion cells are not specialized as transfer cells, indicates that uptake of sucrose by the SE-TCC is primarily, if not entirely, apoplastic. Most importantly, the surface area of the transfer-cell plasmalemma can be experimentally changed by growing plant at different PFDs.

Of course, complex tissue systems are not ideal for analyzing transport across the membrane of a single cell type: there are many potential complications such as disproportional and possibly varying rates of uptake by different cell types and redistribution between cells during the course of the experiment. However, since transfer cells are most often found in complex tissues, and since they are apparently an important component of loading in the intricate tissues of the phloem of certain species, their uptake characteristics must be dealt with in this difficult context. The pea minor veins are at least manageable if morphometric and physiological data are combined.

One of the assumptions we have made in calculating flux is that all loading of sucrose takes place from the apoplast across the SE-TCC plasmalemma. This assumption is based on three lines of evidence. *First*, vein loading of sucrose in *P. sativum* is sensitive to PCMBS (Turgeon and Wimmers 1988), a widely used inhibitor of phloem loading that blocks influx across the plasmalemma from the apoplast (Giaquinta 1983). *Second*, loading of exogenous sucrose occurs directly into the minor veins without being routed through the mesophyll (Turgeon and Wimmers 1988), an indication that the minor veins are capable of preferential uptake of sucrose from the apoplast. The *third* line of evidence, from the work presented here, is that the frequency of plasmodesmata between the SE-TCC and surrounding cells is so low as to cast doubt on the efficacy of a symplastic pathway. In fact, this is not a straightforward argument: we have shown that in any species the frequency of plasmodesmata is expected to decline from the mesophyll toward the minor-vein phloem to compensate for changes in the surface-area to volume ratio of the various tissue types even if the pathway of solute diffusion is entirely symplastic (Ding et al. 1988; Turgeon and Beebe 1991). Therefore, low plasmodesmatal frequency at the SE-TCC boundary is, in itself, not convincing evidence for an apoplastic pathway. However, when compared with data from other species, plasmodesmata at this interface in *P. sativum* are seen to be especially sparse (Table 7).

In Table 7, species are ranked in order of plasmodesmatal frequency at the companion-cell–phloem-parenchyma, and companion-cell–bundle-sheath interfaces. Both absolute and relative frequencies are given since comparisons bases on absolute frequencies suffer from the fact that plasmodesmatal structure and pore size could differ significantly between species, requiring proportionately more or fewer plasmodesmata for the same solute flux. For example, the frequency at all interfaces in *Populus deltoides* are at least twice those reported at

the same interfaces in the other five species. We circumvented this difficulty by calculating relative frequencies based on the phloem-parenchyma–phloem-parenchyma interface as standard (equal to 1.0); this interface has a consistently high frequency of plasmodesmata in the species reported to date. *Coleus blumei* is listed twice since the minor-vein phloem has both 'ordinary' companion cells and intermediary cells (Fisher 1986). Intermediary cells are large, specialized companion cells connected to the bundle sheath by large numbers of plasmodesmata (Turgeon et al. 1975; Turgeon 1989).

In general, the symplast of the sieve-element–companion-cell complex (SE-CCC) is relatively isolated from that of surrounding cells (Table 7) with the notable exceptions of *Populus deltoides* and, especially, the intermediary-cell–bundle-sheath interface of *Coleus blumei*. The SE-CCC symplast is most isolated in *P. sativum* and *Vicia faba*, the two species in which the companion cells are specialized as transfer cells.

Plasmodesmatal frequencies are especially low in *Vicia faba* at almost all interfaces, even in comparison to *P. sativum* (Table 7). These differences in species that belong to the same family, and have the same transfer-cell specialization, underscore the difficulty in comparing plasmodesmatal frequencies (Fisher 1990). When relative frequencies are compared (phloem parenchyma–phloem parenchyma = 1.0), symplastic continuity at the critical interface between the companion (transfer) cell and bundle sheath in *Vicia faba* is not so low as it would otherwise appear, based on absolute frequencies. Indeed, relative frequencies are lower in both *P. sativum* and *Coleus blumei*.

Undoubtedly the most striking differences between species are those at the bundle-sheath–companion-cell boundary, the most likely phloem-loading route, when relative frequencies are assessed. This value for *Coleus blumei* (intermediary cells) is approximately *two orders of magnitude* higher than the value for the two species with transfer cells. While issue can be taken as to subtle differences that exist between plants, this difference obviously supports the opinion that loading of photoassimilate into the SE-CCC may take place along an apoplastic route in some species and a symplastic route in others. This concept has been explored in depth by Gamalei (1985a, b) in a survey of over 170 species in 56 families.

The role of the minor-vein phloem parenchyma should also be considered. In *P. sativum*, phloem-parenchyma cells are often in direct contact with both bundle-sheath and transfer cells and could, therefore, be part of the loading pathway. The plasmodesmatal frequency between phloem-parenchyma cells is very high. Frequencies between phloem-parenchyma and bundle-sheath cells are intermediate in value and there is a low but significant number of plasmodesmata between phloem-parenchyma and transfer cells. However, the tiered arrangement of the parenchyma and SE-TCCs could be a reflection of another function of the phloem parenchyma: to transfer assimilates between SE-TCCs within the same vein.

In summary, while the evidence is circumstantial, it strongly indicates that loading occurs primarily, and perhaps entirely, from the apoplast of the minor vein into the SE-TCC. We feel reasonably secure in making this assumption in our calculations.

A second difficulty in making our flux calculations is that of determining the percentage of exogenous, labeled sucrose that enters the SE-TCC, as opposed to other cell types. To determine what this percentage is we conducted quantitative autoradiography and translocation experiments. Approximately two-thirds of the label from exogenous sucrose is localized in the minor-vein network at the end of uptake studies. Some of this label could have entered the mesophyll before it was subsequently transported to the phloem. This does not seem to be a major factor however; previous studies indicate that exogenous sucrose is taken up directly and preferentially by the minor veins of pea leaves (Turgeon and Wimmers 1988) and, in any case, passage of some label through the mesophyll will not affect the calculations if it is assumed that this label once again enters the apoplast before it is taken up by the SE-TCC. Although errors in measuring the proportion of label taken up by minor veins could have been introduced by the quantitative autoradiography technique, the fact that this proportion was the same in low- and high-light plants tends to minimize errors in comparisons of the two plant groups. Translocation experiments confirmed that approx. 70% of the label applied as exogenous [^{14}C]sucrose enters the translocation stream. Therefore, in calculations of uptake rates it was assumed that two-thirds of the [^{14}C]sucrose accumulated by leaf discs entered the SE-TCC.

Concentration isotherms for sucrose uptake in pea leaf discs consist of saturable and linear components as is typically the case in other species (Maynard and Lucas 1982). Inhibition of saturable uptake by alkaline solutions and PCMBS (data not shown) indicate that the saturable component is probably identical to the carrier-mediated sucrose-proton cotransport system that has been extensively studied (Giaquinta 1983).

The rate of sucrose uptake in leaf discs declines as the leaf expands and begins to export. This is not surprising since the tissue is more compact when immature and sucrose uptake is a feature of plant cells in general, not only exporting tissue. In high-light leaves the decline in rate of uptake with age is not as pronounced as in low-light leaves so that, when mature, the uptake capacity of the former is greater than that of the latter. Sovonick et al. (1974) found that uptake values for sink and source tissues are similar, as we found here in high-light leaves.

Does the greater surface area of the SE-TCC plasmalemma in high-light plants increase the net influx of sucrose from solution? Our evidence indicates that it does. Leaf discs from high-light plants accumulate approx. 50% more exogenous sucrose than those from low-light plants at sucrose concentrations up to 200 mM. By comparison, the surface area of the SE-TCC is 47% greater in low-light than in high-light plants. The transport capacity of both the saturable and linear components of influx increase to approximately the same extent.

Since the proportion of label entering the mesophyll and minor veins is the same in both plant groups, net influx of sucrose must increase in the mesophyll as well as the vascular tissue in high-light plants. Morphometric data indicate that leaves from high-light plants are thicker, intercellular spaces between mesophyll cells are smaller, and there is 47% more mesophyll volume than in low-light leaves (Table 1). This indicates that an increase in mesophyll plasmalemma surface-area or cell volume is responsible for the greater uptake in that tissue. This explanation does not suffice for the minor veins, however. Minor-vein length, cross-sectional area of the SE-TCC, and phloem volume per unit area of leaf surface are the same in low- and high-light plants (Table 1). The only obvious distinguishing feature of the minor veins of the two plant groups that could account for increased net solute influx in high-light leaves is the increase in surface area of the SE-TCC plasmalemma.

Calculated rates of net sucrose influx per unit area of SE-TCC plasmalemma are almost identical in low- and high-light leaves at sugar concentrations below 150 mM. The simplest explanation for this is that increased solute uptake is entirely the consequence of increased plasmalemma area and that the number of carriers per unit plasmalemma area is the same in both low- and high-light leaves. It should be recognized, however, that the complexity of the system and the assumptions required in the calculations do not permit fine distinctions to be made on the density of carriers. For example, ingrowths could provide a microenvironment for localized and steep reduction in apoplast pH, leading to increased uptake, without an increase in carrier number. The proportional increase in linear uptake in high-light leaves indicates that this rate also remains the same per unit area of membrane.

We also measured photoassimilate (as opposed to exogenous sucrose) transport into the phloem transport stream in leaves of low- and high-light plants to determine whether this rate is proportional to SE-TCC plasmalemma area. Translocation rates, and hence transmembrane flux, were calculated from net carbon-exchange data over a 24-h period based on the simplification that carbohydrate is stored during the light period and the rate of export remains approximately the same throughout the day and night. Given this assumption, the increase in transmembrane flux across the SE-TCC in high-light leaves is greater than the increase in plasmalemma surface area (Table 6). In reality, the translocation rate in most plants drops markedly at night (Fondy and Geiger 1982; Huber et al. 1985; Gordon 1986). That drop may be greater in plants adapted to high-light conditions (Gordon 1986). If this is true in pea, our data lead to an underestimate of the difference in SE-TCC transmembrane flux between high- and low-light leaves during the day.

There are several possible explanations for the observation that the increase in flux of endogenous photoassimilate is greater than the increase in plasmalemma surface area. The first is that the apoplastic concentration of sucrose is low enough in low-light plants that carriers are unsaturated and therefore a substantial increase in export sugar does not require a proportional increase in carrier number (plasmalemma surface area). This seems unlikely; uptake rates for exogenous sucrose across the SE-TCC plasmalemma that will account for the amount of sucrose translocated by low-light leaves requires an apoplastic concentration of 50 mM, above the level of sucrose at which the carrier is saturated. Another possibility is that our conclusion concerning the number of carriers per unit area of membrane is incorrect and there is, in fact, a greater density of carriers on the SE-TCC plasmalemma in high-light leaves. A third possibility is that wall ingrowths create a 'standing osmotic gradient' in attached leaves. According to this concept, if solute is rapidly removed from the apex of a wall ingrowth by transport across the adjacent plasmalemma, and by subsequent export, a mass flow of solution toward the apex will result and this will overcome the limitation of diffusion through the wall (Gunning and Pate 1969; Hill 1975a). This effect would be greater in high-light leaves than in low-light leaves since wall ingrowths are more extensive in the former. A standing osmotic gradient would presumable not be created by exogenous sugars in leaf discs since the accumulated sugar in the SE-TCC is not swept away by export.

No matter how this discrepancy between rates of uptake of exogenous sucrose and endogenous photoassimilate is resolved, it is clear that experimental modification of SE-TCC plasmalemma area by altering PFD is accompanied by corresponding changes in the rate of sucrose transport into the cells. The results support experimentally the hypothesis that wall ingrowths in minor-vein transfer cells facilitate uptake of photoassimilate by increasing plasmalemma surface area.

This research was supported by National Science Foundation Grant DCB-9104159, U.S. Department of Agriculture Competitive Grant 90000854, and Hatch funds.

References

Bentwood, B.J., Cronshaw, J. (1978) Cytochemical localization of adenosine triphosphatase in the phloem of *Pisum sativum* and its relation to the function of transfer cells. Planta **140**, 111–120

Bourquin, S., Bonnemain, J.-L., Delrot, S. (1990) Inhibition of loading of ^{14}C assimilates by *p*-chloromercuribenzenesulfonic acid. Localization of the apoplastic pathway in *Vicia faba*. Plant Physiol. **92**, 97–102

Daniel, W.W. (1978) Biostatistics: a foundation for analysis in the health sciences, 2nd edn. Wiley, New York

Ding, B., Parthasarathy, M.V., Turgeon, R. (1988) A morphometric analysis of the phloem-unloading pathway in developing tobacco leaves. Planta **176**, 307–318

Erickson, R.O., Michelini, F.J. (1957) The plastochron index. Am. J. Bot. **44**, 297–305

Evert, R.F., Mierzwa, R.J. (1986) Pathway(s) of assimilate movement from mesophyll cells to sieve tubes in the *Beta vulgaris* leaf. In: Plant biology, vol. 1: Phloem transport, pp. 419–432, Cronshaw, J., Lucas, W.J., Giaquinta, R.T., eds. Alan R. Liss, New York

Faraday, C.D., Thomson, W.W. (1986) Structural aspects of the salt glands of the *Plumbaginaceae*. J. Exp. Bot. **37**, 461–470

Fisher, D.G. (1986) Ultrastructure, plasmodesmatal frequency, and solute concentration in green areas of variegated *Coleus blumei* Benth. leaves. Planta **169**, 141–152

Fisher, D.G. (1990) Distribution of plasmodesmata in leaves. A comparison of *Cananga odorata* with other species using different measures of plasmodesmatal frequency. In: Parallels in cell to cell junctions in plants and animals, pp. 199–221, Robards, A.W., ed. Springer-Verlag, Berlin Heidelberg

Fisher, D.G., Evert, R.F. (1982) Studies on the leaf of *Amaranthus retroflexus* (Amaranthaceae): ultrastructure, plasmodesmatal frequency, and solute concentration in relation to phloem loading. Planta **155**, 377–387

Folsom, M.W., Cass, D.D. (1986) Changes in transfer cell distribution in the ovule of soybean after fertilization. Can. J. Bot. **64**, 965–972

Folsom, M.W., Peterson, C.M. (1984) Ultrastructural aspects of the mature embryo sac of soybean, *Glycine max* (L.) Merr. Bot. Gaz. **145**, 1–10

Fondy, B.R., Geiger, D.R. (1982) Diurnal pattern of translocation and carbohydrate metabolism in source leaves of *Beta vulgaris* L. Plant Physiol. **70**, 671–676

Gamalei, Y.V. (1985a) Plasmodesmata: intercellular communication in plants. [In Russ.] Fiziol. Rast. **32**, 176–190

Gamalei, Y.V. (1985b) Characteristics of phloem loading in woody and herbaceous plants. [In Russ.] Fiziol. Rast. **32**, 866–875

Giaquinta, R.T. (1983) Phloem loading of sucrose. Annu. Rev. Plant Physiol. **34**, 347–387

Gordon, A.J. (1986) Diurnal patterns of photosynthate allocation and partitioning among sinks. In: Phloem transport, pp. 499–517, Cronshaw, J., Lucas, W.J., Giaquinta, R.T., eds. Alan R. Liss, New York

Gunning, B.E.S., Pate, J.S. (1969) "Transfer cells" plant cells with wall ingrowths, specialized in relation to short distance transport of solutes – their occurrence, structure, and development. Protoplasma **68**, 107–133

Gunning, B.E.S., Pate, J.S. (1974) Transfer cells. In: Dynamic aspects of plant ultrastructure, pp. 441–480, Robards, A.W., ed. McGraw-Hill, London, New York

Gunning, B.E.S., Pate, J.S., Briarty, L.G. (1968) Specialized "transfer cells" in minor veins of leaves and their possible significance in phloem translocation. J. Cell Biol. **37**, C7–12

Gunning, B.E.S., Pate, J.S., Minchin, F.R., Marks, I. (1974) Quantitative aspects of transfer cell structure in relation to vein loading in leaves and solute transport in legume nodules. Symp. Soc. Exp. Biol. **28**, 87–126

Hill, A.E. (1975a) Solute-solvent coupling in epithelia; a critical examination of the standing-gradient osmotic flow theory. Proc. R. Soc. London Ser. B **190**, 99–114

Hill, A.E. (1975b) Solute-solvent coupling in epithelia; an electro-osmotic theory of fluid transfer. Proc. R. Soc. London Ser. **190**, 115–134

Huber, S.C., Kerr, P.S., Kalt-Torres, W. (1985) Regulation of sucrose formation and movement. In: Regulation of carbon partitioning in photosynthetic tissue, pp 199–214, Heath, R.L., Preiss, J., eds. American Society of Plant Physiologists, Rockville, Md., USA

Kramer, D., Anderson, W.P., Preston, J. (1978) Transfer cells in the root epidermis of *Atriplex hastata* L. as a response to salinity: a comparative cytological and X-ray microprobe investigation. Aust. J. Plant Physiol. **5**, 739–747

Kronestedt, E.C., Robards, A.W. (1987) Sugar secretion from the nectary of *Strelitzia*: an ultrastructural and physiological study. Protoplasma **137**, 168–182

Kuo, J. (1983) The nacreous walls of sieve elements in seagrasses. Am. J. Bot. **70**, 159–164

Landsberg, E.C. (1982) Transfer cell formation in the root epidermis: a prerequisite for Fe-efficiency? J. Plant Nutr. **5**, 415–432

Maier, K., Maier, U. (1972) Localization of beta-glycerophosphatase and Mg^{++}-activated adenosine triphosphatase in a moss haustorium, and the relation of these enzymes to the cell wall labyrinth. Protoplasma **75**, 91–112

Maynard, J.W., Lucas, W.J. (1982) A reanalysis of the two-component phloem loading system in *Beta vulgaris*. Plant Physiol. **69**, 734–739

Maze, J., Lin, S.C. (1975) A study of the mature megagametophyte of *Stipa elmeri*. Can. J. Bot. **53**, 2958–2977

Pate, J.S. (1966) Photosynthesizing leaves and nodulated roots as donors of carbon to protein of the shoot of the field pea (*Pisum arvense* L.) Ann. Bot. **30**, 93–109

Pate, J.S., Gunning, B.E.S. (1969) Vascular transfer cells in Angiosperm leaves: A taxonomic and morphological survey. Protoplasma **68**, 135–156

Peterson, R.L., Yeung, E.C. (1975) Ontogeny of phloem transfer cells in *Hieracium floribundum*. Can. J. Bot. **53**, 2745–2758

Renault, S., Despeghel-Caussin, C., Bonnemain, J.-L., Delrot, S. (1989) The proton electrochemical transmembrane gradients generated by the transfer cells of the haustorium of *Polytrichum formosum* and their use in the uptake of amino acids. Plant Physiol. **90**, 913–920

Robards, A.W. (1976) Plasmodesmata in higher plants. In: Intercellular communication in plants: studies on plasmodesmata, pp. 15–57, Gunning, B.E.S., Robards, A.W., eds. Springer, Berling Heidelberg New York

Russin, W.A., Evert, R.F. (1985) Studies on the leaf of *Populus deltoides* (Salicaceae): ultrastructure, plasmodesmatal frequency and solute concentrations. Am. J. Bot. **72**, 1232–1247

Scheirer, D.C. (1983) Leaf parenchyma with transfer cell-like characteristics in the moss, *Polytrichum commune* Hedw. Am. J. Bot. **70**, 987–992

Schmalstig, J.G., Geiger, D.R. (1985) Phloem unloading in developing leaves of sugar beet. I. Evidence for pathway through the symplast. Plant Physiol. **79**, 237–241

Schnepf, E. (1974) Gland cells. In: Dynamic aspects of plant ultrastructure, pp. 331–357, Robards, A.W., ed. McGraw-Hill, London, New York

Sovonick, S.A., Geiger, D.R., Fellows, R.J. (1974) Evidence for active phloem loading in the minor veins of sugar beet. Plant Physiol. **54**, 886–891

Spurr, A.R. (1969) A low-viscosity epoxy resin embedding medium for electron microscopy. J. Ultrastruct. Res. **26**, 31–43

Sun, D., Wimmers, L.E., Turgeon, R. (1988) Scintillation counting of ^{14}C-labeled soluble and insoluble compounds in plant tissues. Anal. Biochem. **169**, 424–427

Tilton, V.R., Wilcox, L.W., Palmer, R.G. (1984) Postfertilization wandlabrinthe formation and function in the central cell of soybean, *Glycine max* (L.) Merr. (Leguminosae). Bot. Gaz. **145**, 334–339

Turgeon, R. (1987) Phloem unloading in tobacco sink leaves: insensitivity to anoxia indicates a symplastic pathway. Planta **171**, 73–81

Turgeon, R. (1989) The sink-source transition in leaves. Annu. Rev. Plant Physiol. Plant Mol. Biol. **40**, 119–138

Turgeon, R., Beebe, D.U. (1991) The evidence for symplastic phloem loading. Plant Physiol. **96**, 349–354

Turgeon, R., Wimmers, L.E. (1988) Different patterns of vein loading of exogenous [^{14}C]sucrose in leaves of *Pisum sativum* and *Coleus blumei*. Plant Physiol. **87**, 179–182

Turgeon, T., Webb, J.A., Evert, R.F. (1975) Ultrastructure of minor veins of *Curcurbita pepo* leaves. Protoplasma **83**, 217–232

Watson, L., Pate, J.S., Gunning, B.E.S. (1977) Vascular transfer cells in leaves of Leguminosae-Papilionoideae. Bot. J. Linn. Soc. **74**, 123–130

Willemse, M.T.M., Kapil, R.N. (1981) Antipodals of *Gasteria verrucosa* (Liliaceae) – an ultrastructural study. Acta. Bot. Neerl. **30**, 25–32